O'Driscoll et al., http://www.jcb.org/cgi/content/full/jcb.201505104/DC1

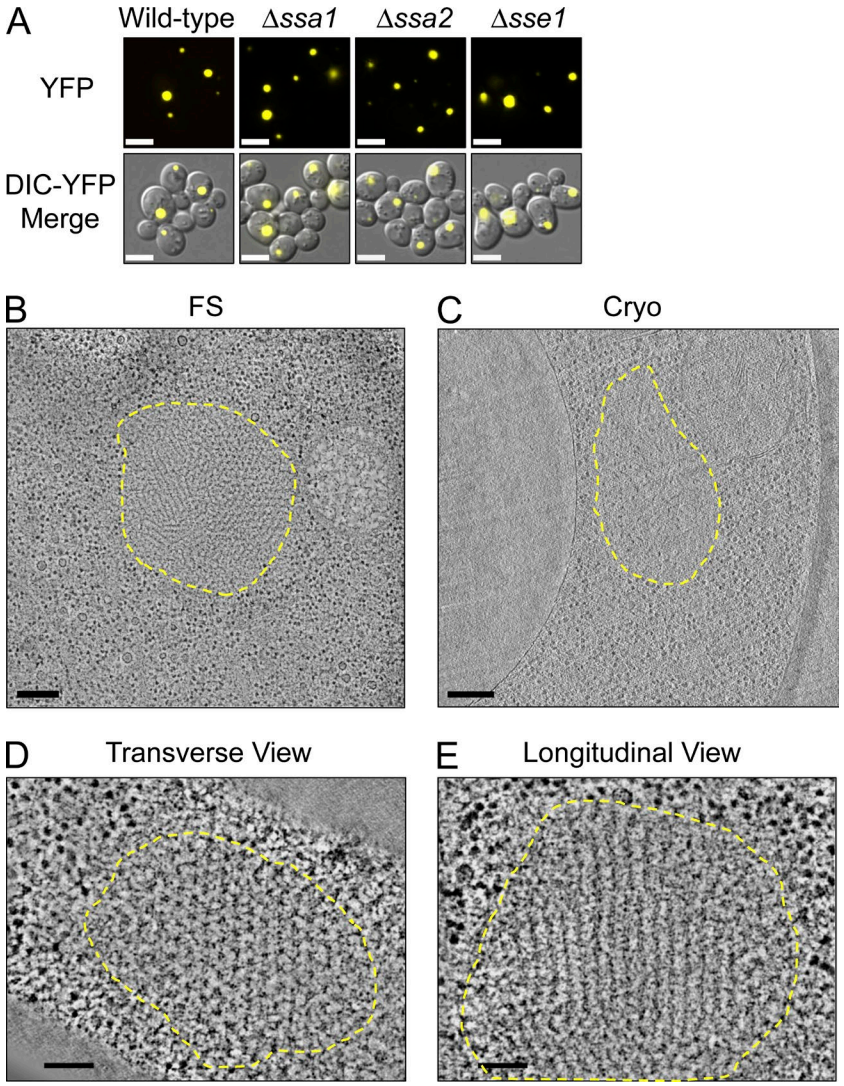

Figure S1. **Live-cell fluorescence microscopy and correlative fluorescence/cryoelectron tomography of NM-YFP dot aggregates.** (A) Live-cell differential interference contrast (DIC) and fluorescence of NM-YFP assemblies in cells with a wild-type chaperone complement and Δ*ssa1*, Δ*ssa2*, and Δ*sse1* gene deletions, as indicated. Bars, 5 µm. (B and C) Representative tomographic slices through reconstructions of NM-YFP dot aggregates from freeze-substituted (FS; B) and vitrified cryosections (Cryo; C), of cells in a wild-type chaperone background. The NM-YFP aggregate is outlined in yellow and manually traced at the interface between the fibrils and the surrounding cytosolic ribosomes. Bars, 200 nm. (D and E) Representative tomographic slices showing transverse (D) and longitudinal (E) views of the fibril arrays in an NM-YFP dot aggregate from freeze-substituted and HM20-embedded material. The NM-YFP aggregate is outlined in yellow, as in B. Bars, 100 nm.

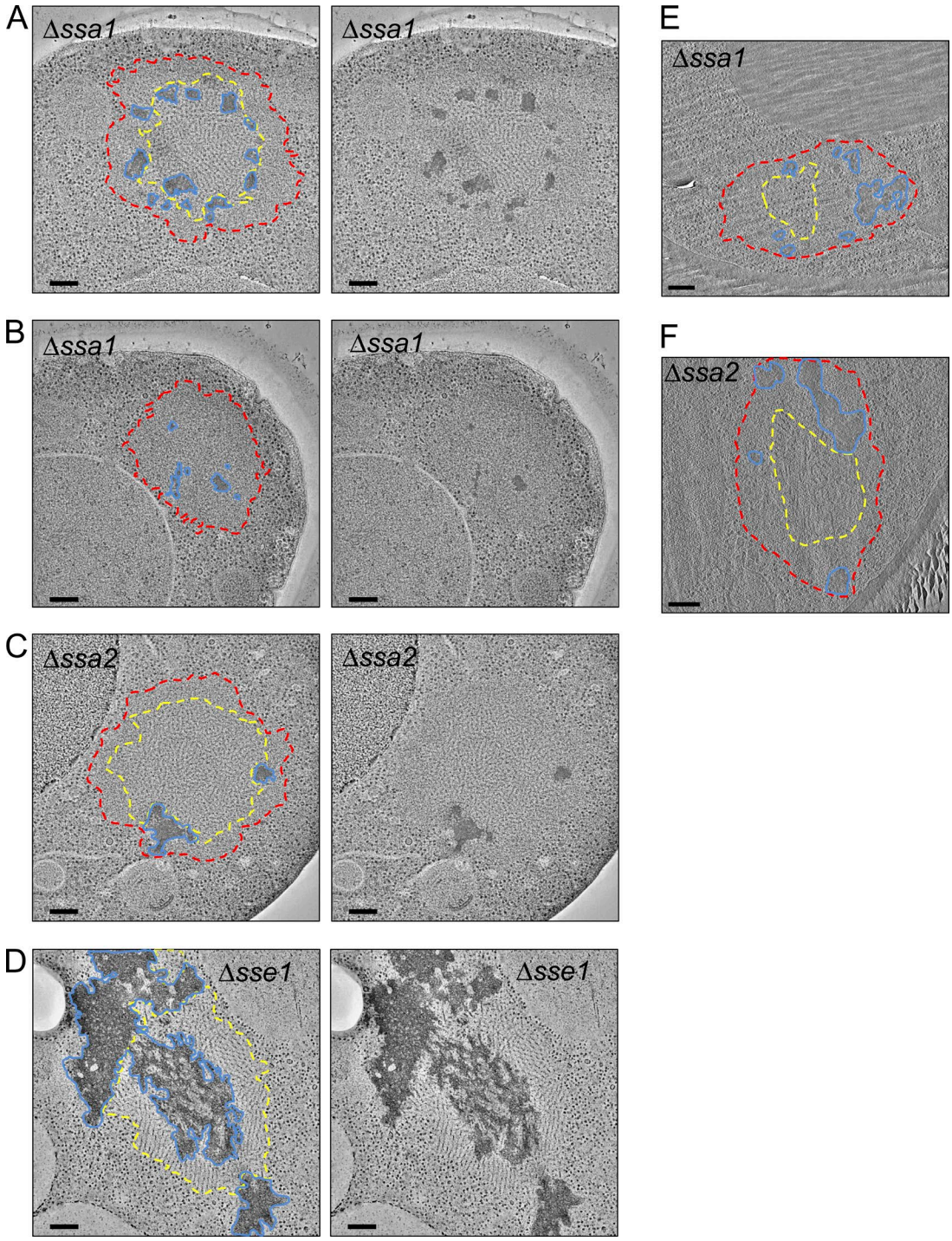

Figure S2. **Aggregate remodelling in Δ*ssa1*, Δ*ssa2*, and Δ*sse1* strains.** Representative tomographic slices through reconstructions of NM-YFP dots in freeze-substituted (Δ*ssa1*, Δ*ssa2*, and Δ*sse1*) and vitreous cryosections (Δ*ssa1* and Δ*ssa2*). (A–D) Tomographic slices are shown with (left) or without (right) annotations. The observed structures were visible in 100% of the aggregates of each respective strain and were from at least 20 independent NM-YFP dot observations (tomograms and projections). Bars, 200 nm. (A) Δ*ssa1*. The NM-YFP aggregate contains fibrils, an unstructured peripheral layer, and dark-staining amorphous aggregates. Fibril-containing regions are outlined in yellow, unstructured perimeter zones are outlined in red, and dark amorphous aggregates are outlined in blue, as described in Fig. 1. (B) Δ*ssa1*. Example of an NM-YFP aggregate consisting entirely of unstructured and dark-staining amorphous aggregates, with no fibril-containing regions. The visible dot regions are outlined as in A. (C) Δ*ssa2*. Annotations are as described in A. (D) Δ*sse1*. The NM-YFP aggregate consists of long fibrils and is accompanied by extensive, darkly stained amorphous aggregates. The fibril-containing region is outlined in yellow and the amorphous aggregates are outlined in blue. (E and F) Representative tomographic slices from cryotomograms of NM-YFP assemblies in vitrified sections of the Δ*ssa1* (E) and Δ*ssa2* (F) strains. The images shown are representative of seven independent NM-YFP assemblies observed in cryo for each of the Δ*ssa1* and Δ*ssa2* strains. The outlines are as described in A.

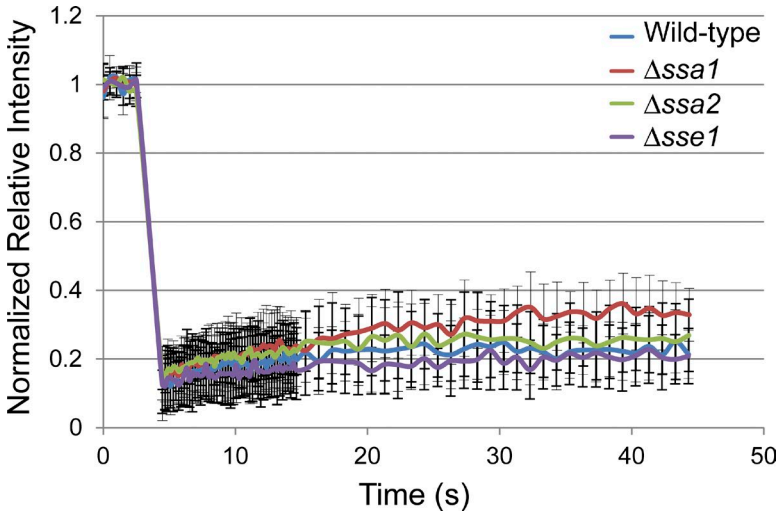

Figure S3. **Molecular mobility in NM-YFP dot aggregates.** FRAP recovery curves for NM-YFP dot aggregates in cells with a wild-type chaperone complement and Δ*ssa1*, Δ*ssa2*, and Δ*sse1* cells as indicated. The data were double normalized to account for differences in starting intensity and bleaching during the time course. The data represents the mean of at least seven independent dot aggregates. Error bars correspond to the SD between the replicates for each time point.

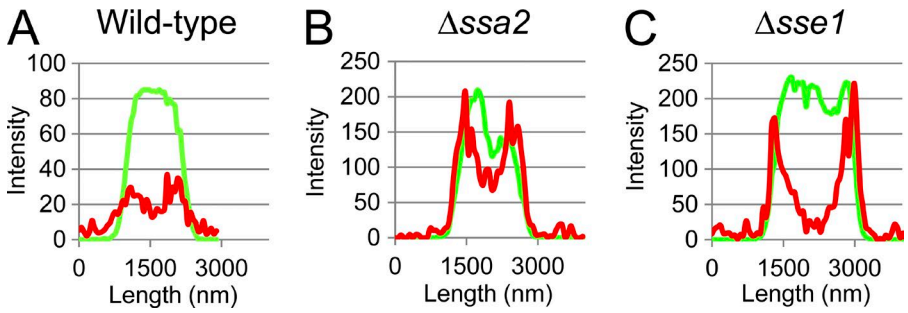

Figure S4. **Distribution of Hsp104-mCherry on NM-YFP aggregate assemblies.** (A–C) Line plots illustrating the colocalization of Hsp104-mCherry (red) with NM-YFP dot aggregates (green) from cells with wild-type chaperone complement (A), Δ*ssa1*(B), or Δ*sse1*(C) deletions, as indicated. The plots were derived from the images shown in Fig. 3 (B–D).

Table S1. **Oligonucleotides used in this study**

Name	Description	Sequence
Δ*SSA1*Fwd	5′ *SSA1* KO	5′-*GTATTACAAGAAACAAAAATTCAAGTAAATAACAGATAATATG*TAGCTTGCCTCGTCCCCGCC-3′
Δ*SSA1*Rev	3′ *SSA1* KO	5′-*AAAGACATTTTCGTTATTATCAATTGCCGCACCAATTGGCTTA*GCCGCATAGGCCACTAGTGG-3′
Δ*SSA2*Fwd	5′ *SSA2* KO	5′-*CCAACAGATCAAGCAGATTTTATACAGAAATATTTATACAATG*TAGCTTGCCTCGTCCCCGCC-3′
Δ*SSA2*Rev	3′ *SSA2* KO	5′-*AGTAAAACTTTTCGGATATTTTACAGGGCGATCGCTAAGCTTA*GCCGCATAGGCCACTAGTGG-3′
Δ*SSE1*Fwd	5′ *SSE1* KO	5′-*TAAGCAAAAAGTACATTGACAAACAACATTTCTTTAAAAGATG*TAGCTTGCCTCGTCCCCGCC-3′
Δ*SSE1*Rev	3′ *SSE1* KO	5′-*ACAATAAAGATCCTTTTCTAGTTACTTTGCTGCATTAACATTA*GCCGCATAGGCCACTAGTGG-3′
HSP104-Cterm_mchFwd	5′ mCherry tag	5′-*GATGACGATAATGAGGACAGTATGGAAATTGATGATGACCTAGATG*GTCGACGGATCCCCGGG-3′
HSP104-Cterm_mchRev	3′ mCherry tag	5′-*TACTGATTCTTGTTCGAAAGTTTTTAAAAATCACACTATATTAAA*GCCGCATAGGCCACTAGTGG-3′
SSA1-Cterm_mch Fwd	5′ mCherry tag	5′-*CCTCCAGCTCCAGAGGCTGAAGGTCCAACCGTTGAAGAAGTTGATG*GTCGACGGATCCCCGGG-3′
SSA1-Cterm_mch Rev	3′ mCherry tag	5′-*CATTAAAAGACATTTTCGTTATTATCAATTGCCGCACCAATTGGC*GCCGCATAGGCCACTAGTGG-3′
SSA2-Cterm_mch Fwd	5′ mCherry tag	5′-*CCTCCAGCTCCAGAAGCTGAAGGTCCAACTGTCGAAGAAGTTGATG*GTCGACGGATCCCCGGG-3′
SSA2-Cterm_mch Rev	3′ mCherry tag	5′-*GCAAAAGTAAAACTTTTCGGATATTTTACAGGGCGATCGCTAAGC*GCCGCATAGGCCACTAGTGG-3′
SIS1-Cterm_mch Fwd	5′ mCherry tag	5′-*ATATCACTAAACGACGCTCAAAAACGTGCTATAGATGAAAATTTTG*GTCGACGGATCCCCGGG-3′
SIS1-Cterm_mch Rev	3′ mCherry tag	5′-*GATAAATTTATTTGAGTTTATAATTATATTTGCTTAGGATTACTA*GCCGCATAGGCCACTAGTGG-3′
pSse1Fwd	5′ *SSE1* cloning	5′-GGGCCCggatccAAAATGAGTACTCCATTTGGTTTAGATTTAG-3′
pSse1Rev	3′ *SSE1* cloning	5′-GGGCCCgtcgacTTAGTCCATGTCAACATCACCTTCAG-3′
pHsp104Fwd	5′ HSP104 cloning	5′-GGGCCCggatccAAAATGAACGACCAAACGCAATTTACAG-3′
pHsp104Rev	3′ HSP104 cloning	5′-GGGCCCgtcgacTTAATCTAGGTCATCATCAATTTCCATAC-3′

Flanking homology is shown in italics and the BamHI and SalI sites are shown in lowercase type. Fwd, forward; KO, knockout; Rev, reverse.